



Computational investigation of single-wall carbon nanotube functionalized with palladium nanoclusters as hydrogen sulfide gas sensor

S. Bagherzadeh-Nobari¹ · K. Hosseini-Istadeh² · R. Kalantarinejad³ · S. M. Elahi¹ · A. A. Shokri⁴

Received: 23 October 2017 / Accepted: 5 February 2018 / Published online: 12 March 2018
© The Author(s) 2018

Abstract

Our aim is to study theoretically, the sensitivity of a hydrogen sulfide gas sensor, with regard to electrical conductance behavior. Our sensor consists of a semiconductor single-wall carbon nanotube (SWCNT), functionalized with palladium nanoclusters, sandwiched between two gold electrodes. Initially, we have computed the optimized structure of the sensor, via molecular dynamic simulations. Then by using non-equilibrium Green's function method, combined with density functional theory, the electronic and transport properties of the sensor were calculated, and compared before and after adsorption of H₂S gas, at different bias voltages. The highest sensitivity is achieved at 40 mV bias voltage. In this bias voltage, H₂S gas adsorption causes a significant decrease of current, because as a result of charge transfer from the CNT and palladium nanoclusters, to H₂S gas, majority carriers (electrons) decrease. The results show that CNT decorated with palladium nanoclusters can be a promising candidate in gas-sensorics.

Keywords H₂S gas sensor · Quantum transport · Palladium decorated carbon nanotubes · Charge transfer

Introduction

Hydrogen sulfide (H₂S) gas is one of the most dangerous gases for humans, due to its toxicity, flammability and being colorless [1]. In addition to its poisonous characteristics, it is mandatory to monitor H₂S in various industries, such as coal mining, oil and gas extraction and petrochemical refining. Current commercial sensors work in high temperature, and have disadvantages, such as high cost and high power consumption [2–4]. Therefore, it is necessary to develop a fast and safe method to detect H₂S gas in low concentrations with high sensitivity.

Nowadays, nanomaterials have attracted a lot of attention due to their unique electrical, optical, magnetic and mechanical properties, and many efforts have been made to improve their fabrication [5, 6]. They are a good candidate in various applications, such as gas sensors [7–10], biosensors [11, 12], magnetic [13] and optoelectronic devices [14].

Among them carbon-based materials, such as graphene and carbon nanotubes are promising candidate, for gas sensing solutions due to their inherent properties, such as large surface to volume ratios, size compatibility and capability to provide high sensitivity. They can be used as a channel in a field effect transistor (FET), or as a resistor between two electrodes. In this type of sensor, because of interaction between adsorbed gas molecules and nanomaterials, electrical properties of the device changes and gas molecule can be detected. These sensors, unlike traditional gas sensor, exhibit faster response, higher sensitivity, smaller size and lower working temperature [15–18]. However, the gas sensing response of graphene and carbon nanotubes is weak, due to the strong sp² bonds of the network, characterized by a low chemical reactivity. To overcome this problem and also for designing a sensor with high selectivity, functionalization of their surface is necessary. It is shown that functionalization with metal

✉ R. Kalantarinejad
kalantari@shezan.ir

¹ Plasma Physics Research Center, Science and Research Branch, Islamic Azad University, Tehran, Iran
² Shezan Research and Innovation Centre, No. 25, Innovation 2 St., Pardis Tech Park, Tehran, Iran
³ Aerospace Research Institute, Ministry of Science, Research and Technology, Tehran, Iran
⁴ Department of Physics, Payame Noor University (PNU), Tehran 19395-3697, Iran

nanoparticles, play a crucial role in producing gas sensors with high sensitivity [19–28]. Different experimental and theoretical studies have been performed for functionalization of carbon nanotubes and graphene, with metal nanoparticles, as the gas sensor [29–35]. For example, Yoosefian theoretically showed that intrinsic single wall carbon nanotube (SWCNT), cannot adsorb NH_3 gas molecules suitably, but SWCNT functionalized with palladium (Pd), facilitate adsorption of NH_3 gas, leading to the high selectivity and fast response of the device [33]. Due to charge transfer between gas molecule and Pd, current changes, and detection will be possible. Berahman theoretically investigated the effect of functionalized graphene with Cu nanoparticles, as an H_2S gas sensor, and showed that due to the strong bond between Cu and H_2S and charge transfer from H_2S to Cu, detection is possible [34]. Fam et al. fabricated an H_2S gas sensor, based on SWCNT, decorated with silver nanoparticles. They showed that due to permanent bonding between Ag and S, the current decreases and detection is possible. Their sensor is selective respect to No and Co gases, because the interaction between Ag and H_2S is stronger than interaction between Ag with No and Co. Nevertheless, due to the strong chemical interaction between Ag and H_2S , the sensor is not regenerated [35].

Asad et al. fabricated a flexible H_2S gas sensor, based on SWCNT, decorated with Cu nanoparticles. They showed that due to catalytic properties of Cu, the sensor shows a fast response and recovery time. Also, the sensor is selective, in respect to H_2 , ethanol, acetone and methane gases, and the response of the sensor is reproducible [29].

In this study, we investigated the sensing ability and mechanism of SWCNT, decorated with palladium nanoclusters (Pd-SWCNT), sandwiched between two gold electrodes, as an H_2S gas sensor, as it was reported experimentally by Star et al. [31] that carbon nanotubes decorated with Pd nanoparticles, show better response towards H_2S gas. Our analysis is carried out at the level of density functional theory (DFT) [36], combined with the non-equilibrium Green's function (NEGF) method, for calculation of quantum transport [37].

The rest of the paper is classified as follows: in “**Methods**”, theoretical method and computational details are presented. In “**Results and discussions**”, transport properties of Pd-SWCNT, once with no H_2S molecules in the system [state (a)] and once with H_2S molecules [state (b)] in the system are computed. At first, current and sensitivity of the system in the state (a) and state (b) at different bias voltages, are computed and optimized voltage for the sensor is defined. After that, projected density of states (PDOS), transmission coefficient $T(E)$ at optimized bias voltage for the sensor in the state (a) and (b), are calculated and discussed in details. Then sensing mechanism of sensor is analyzed with calculation of charge transfer by Mulliken Pop analysis. Finally,

in “**Conclusions**” the paper is summarized and followed by conclusions.

Methods

Simulation details

The proposed sensor comprises three major sections, namely a right-hand side and a left-hand side electrode, and the device region or transducer of the sensor. The electrodes are semi-infinite gold (111) crystals, while the device region consists of a functionalized semiconducting (8,0) SWCNT, nearly 100 Å long, with five Au layers on each side. The gap between the SWCNT i.e. Au/CNT/Au junctions and the Au layers was set to 2 Å. Six sites of adsorption, made up of 1 Pd cluster, have been modeled on the CNT. In order to study the behavior of the gas sensor, we first need to find the optimized geometries of the sensor, with having no H_2S and with H_2S molecules in the system. The minimization process has been carried out, for which we use conjugated gradient method [38], and chemical force field, based on AVOGADRO software in the state (a) and (b) [39]. The coordinates of atoms for the optimized geometry have been used, as the input file for SMEAGOL software [40, 41]. Here, we have carried out electrical/quantum transport calculation, using SMEAGOL code, taking advantage of SIESTA [42], as its DFT platform. Hamiltonian and overlap matrices in SMEAGOL, are generated by DFT method. Hereunder, the mathematical equation for constructing Hamiltonian, and overlap matrices is expressed:

$$H_{IJ}^{\alpha\beta} = \langle \varphi^\alpha | H(n) | \varphi^\beta \rangle \quad (1)$$

$$S_{IJ}^{\alpha\beta} = \langle \varphi^\alpha | \varphi^\beta \rangle. \quad (2)$$

In the above equations, α and β represent the SIESTA numerical atomic orbital basis sets, $H(n)$ labels the Hamiltonian operator, and n is the electron density. The ‘partition’ symbolizes I and J , takes the values L, R or D, indicating the left and right electrodes and the sensing region of the device. The core concept in the non-equilibrium Green's function method is the retarded Green's function of the device-sensing region, which reads [41]:

$$G_D^R(E) = \left[\varepsilon^+ S_{DD} - H_{DD} - \sum_L^R(E) - \sum_R^R(E) \right]^{-1} \quad (3)$$

where $\sum_{L,R}^R(E)$ are the electrode self-energies. These can be calculated as:

$$\sum_I^R(E) = (\varepsilon^+ S_{DI} - H_{DI}) G_{II}^R(E) (\varepsilon^+ S_{ID} - H_{ID}) \quad (4)$$

In the Eq. (4), $\epsilon^+ = \lim_{\delta \rightarrow 0^+} E + i\delta$ is the energy, $G_{\Pi}^R(E)$ is the retarded Green’s function of electrodes [38]. The equation includes multiplication of infinite matrices, a closed form for $\Sigma_{L,R}^R(E)$ exists that requires only information about electrodes’ unit cells and the coupling of electrodes’ surface to the device region [41].

The electron density is calculated by the equation below:

$$n(\vec{r}) = \langle \vec{r} | D | \vec{r} \rangle, \tag{5}$$

where, D is the density matrix, which can be written by lesser Green’s function $G_D^<$, [38] as follows:

$$D = \frac{1}{2\pi i} \int G_D^<(E) dE, \tag{6}$$

where, in case equilibrium the lesser Green’s function is

$$G_D^<(E) = -2i \text{Im} [G_D^R(E) f(E - \mu)]. \tag{7}$$

The set of Eqs. (1) to (7) form a set of self-consistent equations, which can be iteratively solved to find G_D^R , since G_D^R yields all the necessary data, to picture the electronic structure of the sensing region, together with electrodes.

The current, passing through the scattering central region is calculated by the Landauer formula [37]:

$$I(V) = \frac{2e^2}{h} \int_{-\infty}^{\infty} T(E, V) [f(E - \mu_L) - f(E - \mu_R)] dE, \tag{8}$$

where, L and R denote left and right electrodes, respectively, $T(E, V)$ is the transmission coefficient, which is a function of the energy and bias voltage (the voltage applied across the electrodes). $f_{L/R}$ is the Fermi–Dirac distribution function and $\mu_{L/R}$ is the electrochemical potential.

In Eq. (8), transmission coefficient is calculated as follows:

$$T = \text{Tr} [\Gamma_L G_D^{R*} \Gamma_R G_D^R], \tag{9}$$

where

$$\Gamma_{L,R}(E) = i \left[\sum_{L,R}^R(E) - \sum_{L,R}^{R*}(E) \right]. \tag{10}$$

We have only made use of minimal basis sets for SWCNT atoms, so that the cost of computation will be low, taking into account the fact that only the states around the Fermi level E_F are the most important to transport property calculations [28]. Similarly, we took d orbital of gold atoms in the core into account and only used the 6 s Shell, as the orbital of the valence band of the gold atoms [11]. For the sulfur atoms in H_2S molecules, S atoms have been brought into computation, by assigning single zeta polarized basis sets, while for the hydrogen atoms, a single zeta basis has been used. For the Pd atoms, also a single zeta basis set has been applied. Exchange–correlation energies have been

calculated, using Local Density Approximation (LDA), in Ceperley–Alder form [43]. The Convergence tolerance, i.e. tolerance in maximum difference, for the density matrix calculation has been set to 10^{-4} . On the other hand the mesh cut-off, which is the equivalent plane-wave energy cut-off for the real-space grid, was set at 200 Ry. We also used $1 \times 1 \times 80$ Monkhorst scheme k-grid of electrodes (the total number of Au atoms in the electrodes’ cell was 144). The super cell size is chosen, to avoid any image-cell interaction. We have used periodic boundary conditions, in the orthogonal direction, in respect to the direction of transport.

Amongst the outputs of the simulation, three files have been obtained: a file containing current voltage points, used to draw the I – V Curve, a second file containing transmission coefficient energy points that can be used to plot transmission as a function of energy, and a third file related to PDOS that must be post-processed by fmpdos utilities of SIESTA to calculate projected density of states over carbon atoms of carbon nanotube. The resulting file can be used to draw PDOS over carbon atoms, as a function of energy.

Results and discussions

In this study, we have investigated the sensing ability of the single wall carbon nanotube, decorated with Pd nanoclusters, as an H_2S gas sensor. For this purpose, we have calculated and compared the electrical properties of the Pd-SWCNT, in the state (a) and (b). Initially, the optimized structure of the sensor in the state (a) and (b) is acquired, by molecular dynamic simulations. The results are presented in Fig. 1. Then the electrical current of the device is calculated in the state (a) and (b), at different bias voltages, and presented in Table 1 and Fig. 2. As presented in Fig. 2, for two states of (a) and (b), the current was increased, with an increment in the amount of bias voltage. Also in constant voltage, adsorption of H_2S gas, caused a significant decrease in the current, consistent with experimental results [31]. In conclusion, we can state that H_2S molecules can alter the conductance of the device considerably, and the sensor can be used, as an experimental sensor.

As seen in Fig. 2, the response of the device to H_2S gas is different, at different bias voltages, so we have calculated the sensitivity of the device at different bias voltages, in order to find the optimized voltage for the sensor.

The sensitivity is determined as follows:

$$S(\%) = \frac{|R - R_0|}{R_0} \times 100, \tag{11}$$

where R_0 and R are the resistivity of device in the state (a) and (b), respectively. Results are presented in Table 1. As presented in Table 1, at 40 mV bias voltage, the sensitivity

Fig. 1 Geometry of the conductometric H_2S sensor, based on carbon nanotube, decorated with Pd groups. Hydrogen atoms (white), sulfur atoms (green), gold electrodes (yellow), CNT (gray) and palladium clusters (purple)

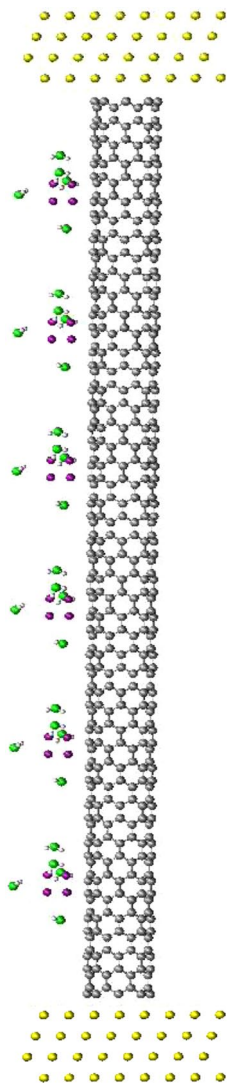


Table 1 Calculated current (μA) and sensitivity at different bias voltages in state (a) and (b)

Voltage(mV)	Current in state (a)	Current in state (b)	Sensitivity
0	0	0	0%
20	0.51	0.42	17.65%
40	1.53	0.89	41.83%
60	2.01	1.48	26.36%

is maximized. Therefore, we have studied the transport properties of the sensor and sensing mechanism, in this bias voltage.

We have calculated the PDOS over the SWCNT and the transmission coefficient of the sensor in the state (a) and (b), as a function of energy at 40 mV bias voltage (Fig. 3a, b, respectively). In all figures, the energy zero is set to the Fermi energy of the Au electrode. Initially, we investigated

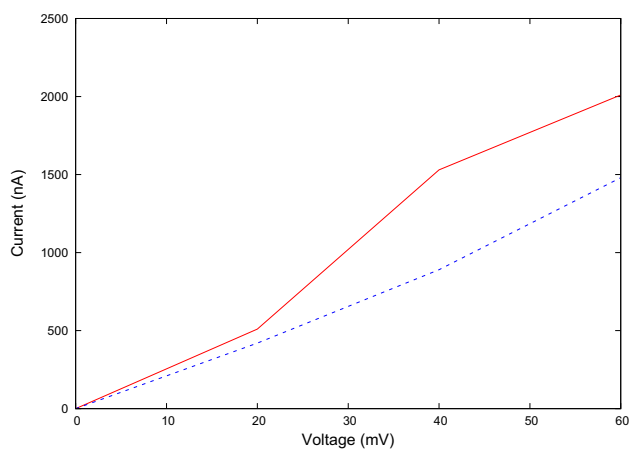


Fig. 2 The current–voltage characteristics for state (a) (solid line) and (b) (dash line)

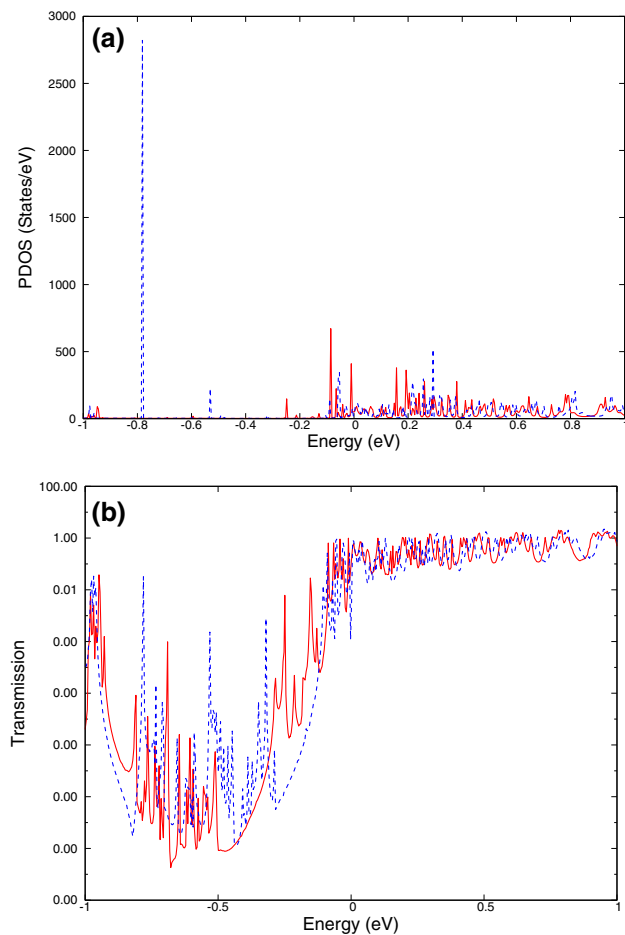


Fig. 3 Electronic and transport properties of the sensor, before (solid line) and after H_2S gas adsorption (dashed line). **a** The projected density of state over CNT, as a function of energy in the state (a) and (b). **b** The related transmission coefficient as a function of energy. Here, $T(E)$ is plotted in logarithmic scale



the results of the case without any H_2S gas molecules (solid line in Fig. 3). As presented in Fig. 3a continuous states, seen in the PDOS diagram relate to the conduction band of the SWCNT, decorated with Pd nanoclusters. We can clearly see that the conduction band edge is at -0.268 eV, below the Fermi level. As a result, the Pd-SWCNT is a degenerate n-type semiconductor. Also, there are some small, localized states at -0.6 and -0.9 eV energies, in the band gap region.

Transmission coefficient, as a function of energy is presented in the Fig. 3b. $T(E)$ is the probability of transmission of one electron, from one to another electrode. There is a good agreement between PDOS and T diagram. As seen in the figure, $T(E)$ increases sharply to about 1, at the onset of the CNT conduction band, placed at -0.268 eV. The presence of localized states, at -0.6 and -0.9 eV in the mid gap region, results in increase of $T(E)$, at that energies and cause mid gap tunneling conductance.

Finally, we analyzed the PDOS and $T(E)$ of the sensor, in the presence of H_2S gas (dashed line in Fig. 3), and compared the results, with no H_2S gas molecules state. As seen in Fig. 3a, after adsorption of H_2S , the conduction band in the PDOS diagram shifts to higher energies. Moreover, due to interaction between Pd-SWCNT and the H_2S gas, new localized states appeared at energies, around -0.5 and -0.78 eV, and some states at energies near the conduction band edge, disappeared. Disappearing of some states at the conduction band edge, and the shift of the conduction band to the higher energies, lead to the shift of the conduction band edge from -0.26 to -0.114 eV. As a result, distance between the Fermi level and the conduction band edge decreased. This effect can be due to reduction of concentration of majority carriers (electrons). Subsequently, we investigated this issue, by calculating the charge density difference in the system.

Change in the PDOS, causes a significant modification in $T(E)$. According to Fig. 3b, after adsorption of H_2S the transmission onset at the CNT conduction band shifts to higher energies from -0.26 to -0.114 eV, due to the disappearance of some states near the conduction band, and the shift of the entire conduction band to higher energies. In the band gap region, the transmission increased significantly at energies around -0.5 and -0.78 eV, due to the presence of localized states in these energies. These mid gap states cause mid gap tunneling conductance, but according to Landauer formula only states in the energy range between -0.02 and 0.02 eV, participate in the current at 40 mV bias voltage. For that reason, appearing of localized states does not affect the current.

Finally, we aim to interpret the reason for the decrement in current, in case of H_2S adsorption. According to Landauer equation, at 40 mV bias voltage, only states in the energy range between ± 0.02 eV, contribute to the current. Therefore, we looked at the PDOS and T in this energy window

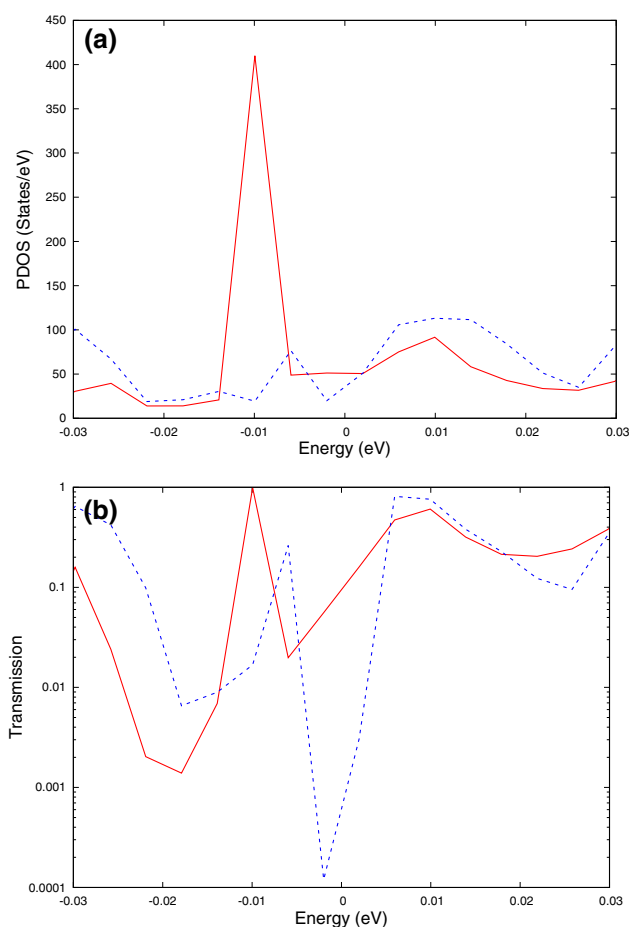


Fig. 4 Electronic and transport properties of the sensor, before (solid line) and after H_2S gas adsorption (dashed line), in the energy window between ± 0.03 eV. **a** The projected density of state over CNT, as a function of energy in the state (a) and (b). **b** The related transmission coefficient as a function of energy. Here, $T(E)$ is plotted in logarithmic scale

(Fig. 4a, b, respectively). As seen in this energy window, the PDOS and consequently T , decrease in this energy range, after H_2S adsorption, and as a result current decrease significantly.

The sensing mechanism and the changes in the PDOS and T , after adsorption of H_2S gas can be rationalized, by calculating charge density by Mulliken Pop analysis. We computed the change in the charge density of the system, when H_2S gas is adsorbed. Charge density difference is defined as follows:

$$\Delta n = n_{\text{Pd-SWCNT}/\text{H}_2\text{S}} - n_{\text{Pd-SWCNT}} - n_{\text{H}_2\text{S}}, \quad (12)$$

where $n_{\text{Pd-SWCNT}/\text{H}_2\text{S}}$, $n_{\text{Pd-SWCNT}}$ and $n_{\text{H}_2\text{S}}$ are the charge density of Pd-SWCNT/ H_2S , Pd-SWCNT and H_2S gas, respectively. The results are presented in Table 2. As seen in Table 2, after adsorption of H_2S charge transfers significantly, from Pd and SWCNT to H_2S molecules. Due to the charge transfer, the concentration of majority carriers in



Table 2 Charge transfer in the system after H₂S adsorption

Element	CNT	Pd	H ₂ S
Excess Charge ΔQ	− 1.787q	− 2.296q	+ 4.083q

SWCNT decreases (because SWCNT decorated with Pd nanoclusters is n-type semiconductor), consistent with previous finding in the PDOS and current–voltage diagrams (distance between the Fermi energy and the conduction band edge decreased and current decreased). Also, as a result of charge transfer, negatively charged H₂S molecules act, as an electrostatic gate and shifts the PDOS, and as a result $T(E)$, to higher energies, consistent with modification of the PDOS diagram and T , after H₂S gas adsorption, as mentioned before. Our results show that the sensor can detect H₂S gas, with high sensitivity at 40 mV bias voltage, due to a significant decrease in the current, after H₂S gas adsorption.

Conclusions

In this study, the effect of adsorption of H₂S gas on electrical properties of single wall carbon nanotube, decorated with Pd nanoclusters, was investigated between two gold electrodes. For this purpose, current at different bias voltages, in the absence and presence of H₂S gas was calculated. Then, sensitivity of the device at different bias voltages was computed and compared. We find that the largest sensitivity takes place at a bias voltage of 40 mV. In this bias voltage, the PDOS and T in two states (a) and (b), are computed, and compared accordingly. After adsorption of H₂S gas, the PDOS and as a result T , were decreased significantly, in the energy window between ± 0.02 eV, leading to a significant decrease in the current, from 1.53 to 0.89 μ A. This reduction is due to the charge transfer from Pd nanoclusters and SWCNT to H₂S gas that results in reduction of concentration of majority carriers (electrons). The results show that carbon nanotube, decorated with Pd nanoclusters can be a promising candidate, for fabrication of FET gas sensors.

Open Access This article is distributed under the terms of the Creative Commons Attribution 4.0 International License (<http://creativecommons.org/licenses/by/4.0/>), which permits unrestricted use, distribution, and reproduction in any medium, provided you give appropriate credit to the original author(s) and the source, provide a link to the Creative Commons license, and indicate if changes were made.

References

- Li, P., Li, J., Zhao, S., Kong, L., Zhai, Y.: Research on the danger of fires in oil tanks with sulfur. *Fire Saf. J.* **40**, 331–338 (2005)
- Verma, M.K., Gupta, V.: A highly sensitive SnO₂–CuO multilayered sensor structure for detection of H₂S gas. *Sens. Actuators B* **166**, 378–385 (2012)
- Zhang, R.H., Zhang, X.T., Hu, S.M.: Novel sensor based on Ag/Ag₂S electrode for in situ measurement of dissolved H₂S in high temperature and pressure fluids. *Sens. Actuators B Chem.* **177**, 163–171 (2013)
- Shao, F., Hoffmann, M.W., Prades, J.D., Zamani, R., Arbiol, J., Morante, J.R.: & Fischer, T.: heterostructured p-CuO (nanoparticle)/n-SnO₂ (nanowire) devices for selective H₂S detection. *Sens. Actuators B Chem.* **181**, 130–135 (2013)
- Ghodselahe, T., Solaymani, S., Akbarzadeh Pasha, M., Vesaghi, M.A.: Ni nanoparticle catalyzed growth of MWCNTs on Cu NPs@ aC: H substrate. *Eur. Phys. J. D* **66**, 299 (2012)
- Țălu, Ș., Bramowicz, M., Kulesza, S., Solaymani, S., Shafikhani, A., Ghaderi, A., Ahmadirad, M.: Gold nanoparticles embedded in carbon film: micromorphology analysis. *J. Ind. Eng. Chem.* **35**, 158–166 (2016)
- Miranda, A., de Santiago, F., Pérez, L.A., Cruz-Irisson, M.: Silicon nanowires as potential gas sensors: a density functional study. *Sens. Actuators B Chem.* **242**, 1246–1250 (2017)
- Feng, P., Shao, F., Shi, Y., Wan, Q.: Gas sensors based on semi-conducting nanowire field-effect transistors. *Sensors*. **14**, 17406–17429 (2014)
- Zhang, J., Liu, X., Neri, G., Pinna, N.: Nanostructured materials for room-temperature gas sensors. *Adv. Mater.* **28**, 795–831 (2016)
- Krepel, D., Peralta, J.E., Scuseria, G.E., Hod, O.: graphene nanoribbons-based ultrasensitive chemical detectors. *J. Phys. Chem. C*. **120**, 3791–3797 (2016)
- Kalantari-Nejad, R., Bahrami, M., Rafii-Tabar, H., Rungger, I., Sanvito, S.: Computational modeling of a carbon nanotube-based DNA nanosensor. *Nanotechnology*. **21**, 445501 (2010)
- Bagherzadeh-Nobari, S., Kalantarinejad, R., Elahi, S.M., Sanvito, S.: Computational investigation of label free detection of biomolecules based on armchair graphene nanoribbon. *Sens. Actuators B Chem.* **255**, 1276–1284 (2018)
- Boochani, A., Nowrozi, B., Khodadadi, J., Solaymani, S., Jalali-Asadabadi, S.: Novel graphene-like Co₂VAI (111): case Study on magnetoelectronic and optical properties by first-principles calculations. *J. Phy. Chem. C*. **121**, 3978–3986 (2017)
- Lashgari, H., Boochani, A., Shekaari, A., Solaymani, S., Sartipi, E., Mendi, R.T.: Electronic and optical properties of 2D graphene-like ZnS: FFT calculations. *Appl. Surf. Sci.* **369**, 76–81 (2016)
- Oftadeh, M., Gholamian, M., Abdallah, H.H.: Investigation of interaction hydrogen sulfide with (5, 0) and (5, 5) single-wall carbon nanotubes by density functional theory method. *Int. Nano Lett.* **3**, 7 (2013)
- Mishra, P., Islam, S.S.: Trace level ammonia sensing by SWCNTs (network/film) based resistive sensor using a simple approach in sensor development and design. *Int. Nano Lett.* **3**, 46 (2013)
- Moradian, R., Nazeri, S.: Retracted: electrical conductivity of hydrogenated armchair nanoribbon as a gas sensor using non-equilibrium Green's function method. *Int. Nano Lett.* **2**(1), 3 (2012)
- Li, J., Lu, Y., Ye, Q., Cinke, M., Han, J., Meyyappan, M.: Carbon nanotube sensors for gas and organic vapor detection. *Nano Lett.* **3**, 929–933 (2003)
- Zhao, Q., Buongiorno Nardelli, M., Lu, W., Bernholc, J.: Carbon nanotube—metal cluster composites: anew road to chemical sensors? *Nano Lett.* **5**, 847–851 (2005)
- Aroutiounian, V.M.: Gas sensors based on functionalized carbon nanotubes. *J. Contemp. Phys. (Armenian Academy of Sciences)* **50**, 333–354 (2015)
- Cui, S., Pu, H., Lu, G., Wen, Z., Mattson, E.C., Hirschmugl, C., Chen, J.: Fast and selective room-temperature ammonia sensors

- using silver nanocrystal-functionalized carbon nanotubes. *ACS Appl. Mater. Interfaces*. **4**, 4898–4904 (2012)
22. Dube, I., Jiménez, D., Fedorov, G., Boyd, A., Gayduchenko, I., Paranjape, M., Barbara, P.: Understanding the electrical response and sensing mechanism of carbon-nanotube-based gas sensors. *Carbon* **87**, 330–337 (2015)
 23. Zanolli, Z., Leghrib, R., Felten, A., Pireaux, J.J., Llobet, E., Charlier, J.C.: Gas sensing with Au-decorated carbon nanotubes. *ACS Nano* **5**, 4592–4599 (2011)
 24. Colindres, S.C., Aguir, K., Cervantes Sodi, F., Vargas, L.V., Salazar, J.A.M., Febles, V.G.: Ozone sensing based on palladium decorated carbon nanotubes. *Sensors*. **14**, 6806–6818 (2014)
 25. Zhang, X., Gui, Y., Dai, Z.: A simulation of Pd-doped SWCNTs used to detect SF₆ decomposition components under partial discharge. *Appl. Surf. Sci.* **315**, 196–202 (2014)
 26. Abdelhalim, A., Winkler, M., Loghin, F., Zeiser, C., Lugli, P., Abdallah, A.: Highly sensitive and selective carbon nanotube-based gas sensor arrays functionalized with different metallic nanoparticles. *Sens. Actuators B Chem.* **220**, 1288–1296 (2015)
 27. Mubeen, S., Zhang, T., Yoo, B., Deshusses, M.A., Myung, N.V.: Palladium nanoparticles decorated single-walled carbon nanotube hydrogen sensor. *J. Phys. Chem. C*. **111**, 6321–6327 (2007)
 28. Cao, C., Kemper, A.F., Agapito, L., Zhang, J.W., He, Y., Rinzier, A., Sanvito, S.: Nonequilibrium Green's function study of Pd₄-cluster-functionalized carbon nanotubes as hydrogen sensors. *Phys. Rev. B*. **79**, 075127 (2009)
 29. Asad, M., Sheikhi, M.H., Pourfath, M., Moradi, M.: High sensitive and selective flexible H₂S gas sensors based on Cu nanoparticle decorated SWCNTs. *Sens. Actuators B Chem.* **210**, 1–8 (2015)
 30. Mubeen, S., Zhang, T., Chartuprayoon, N., Rheem, Y., Mulchandani, A., Myung, N.V., Deshusses, M.A.: Sensitive detection of H₂S using gold nanoparticle decorated single-walled carbon nanotubes. *Anal. Chem.* **82**, 250–257 (2009)
 31. Star, A., Joshi, V., Skarupo, S., Thomas, D., Gabriel, J.C.P.: Gas sensor array based on metal-decorated carbon nanotubes. *J. Phys. Chem. B* **110**, 21014–21020 (2006)
 32. Zhang, X., Dai, Z., Wei, L., Liang, N., Wu, X.: Theoretical calculation of the gas-sensing properties of Pt-decorated carbon nanotubes. *Sensors*. **13**, 15159–15171 (2013)
 33. Yoosefian, M.: Powerful greenhouse gas nitrous oxide adsorption onto intrinsic and Pd doped Single walled carbon nanotube. *Appl. Surf. Sci.* **392**, 225–230 (2017)
 34. Berahman, M., Sheikhi, M.H.: Hydrogen sulfide gas sensor based on decorated zigzag graphene nanoribbon with copper. *Sens. Actuators B Chem.* **219**, 338–345 (2015)
 35. Fam, D.W.H., Tok, A.I.Y., Palaniappan, A., Noppawan, P., Lohani, A., Mhaisalkar, S.G.: Selective sensing of hydrogen sulfide using silver nanoparticle decorated carbon nanotubes. *Sens. Actuators B Chem.* **138**, 189–192 (2009)
 36. Hohenberg, P., Kohn, W.: Inhomogeneous electron gas. *Phys. Rev.* **136**, B864 (1964)
 37. Datta, S.: *Electronic transport in mesoscopic systems*. Cambridge University Press, Cambridge (1995)
 38. Rocha, A.R., Garcia-Suarez, V.M., Bailey, S.W., Lambert, C.J., Ferrer, J., Sanvito, S.: Towards molecular spintronics. *Nat. Mater.* **4**, 335 (2005)
 39. Rungger, I., Sanvito, S.: Algorithm for the construction of self-energies for electronic transport calculations based on singularity elimination and singular value decomposition. *Phys. Rev. B*. **78**, 035407 (2008)
 40. Soler, J.M., Artacho, E., Gale, J.D., García, A., Junquera, J., Ordejón, P., Sánchez-Portal, D.: The SIESTA method for ab initio order-N materials simulation. *J. Phys. Condens. Matter* **14**, 2745 (2002)
 41. Sanvito, S., Lambert, C.J., Jefferson, J.H., Bratkovsky, A.M.: General Green's-function formalism for transport calculations with spd Hamiltonians and giant magnetoresistance in Co- and Ni-based magnetic multilayers. *Phys. Rev. B*. **59**, 11936 (1999)
 42. Toher, C., Sanvito, S.: Effects of self-interaction corrections on the transport properties of phenyl-based molecular junctions. *Phys. Rev. B*. **77**, 1554 (2008)
 43. Ceperley, D.M., Alder, B.J.: Ground state of the electron gas by a stochastic method. *Phys. Rev. Lett.* **45**, 566 (1980)

Publisher's Note Springer Nature remains neutral with regard to jurisdictional claims in published maps and institutional affiliations.

